In-Phantom Measurements of the Bremsstrahlung Dose for Megavoltage Electron Beams Incident on Metals for Use in an electron Multileaf Collimator

Chester S. Reft
Department of Radiation Oncology
University of Chicago Medical Center

Dosimetry of a prototype retractable eMLC for fixed-beam electron therapy

Kenneth R. Hogstrom,[a] Robert A. Boyd, and John A. Antolak
Department of Radiation Physics, The University of Texas M. D. Anderson Cancer Center, Houston, Texas 77030

Michelle M. Svatos
Oncology Care Systems, Siemens Medical Solutions USA, Inc., Concord, California 94520

Bruce A. Faddegon
Department of Radiation Oncology, University of California San Francisco, San Francisco, California 94143

Julian G. Rosenman
Department of Radiation Oncology, University of North Carolina, Chapel Hill, North Carolina 27599

(Received 22 July 2003; revised 25 November 2003; accepted for publication 26 November 2003; published 6 February 2004)

An electron multileaf collimator (eMLC) has been designed that is unique in that it retracts to 37 cm from the isocenter [63-cm source-to-collimator distance (SCD)] and can be deployed to distances of 20 and 10 cm from the isocenter (80 and 90 cm SCD, respectively). It is expected to be capable of arc therapy at 63 cm SCD; isocentric, fixed-beam therapy at 80 cm SCD; and source-to-surface distance (SSD), fixed-beam therapy at 90 cm SCD. In all positions, its leaves could be used for unmodulated or intensity-modulated therapy. Our goal in the present work is to describe the general characteristics of the eMLC and to demonstrate that its leakage characteristics and dosimetry are adequate for SSD, fixed-beam therapy as an alternative to Cerrobend cutouts with applicators once the prototype's leaves are motorized. Our eMLC data showed interleaf electron leakage at 15 MeV to be less than 0.1% based on a 0.0025 cm manufacturing tolerance, and lateral electron leakage at 5 and 15 MeV to be less than 2%. X-ray leakage through the leaves was 1.6% at 15 MeV. Our data showed that beam penumbra was independent of direction and leaf position. The dosimetric properties of square fields formed by the eMLC were very consistent with those formed by Cerrobend inserts in the 20×20 cm^2 applicator. Output factors exhibited similar field-size dependence. Airgap factors exhibited almost identical field-size dependence at two SSDs (105 and 110 cm), consistent with the common assumption that airgap factors are applicator independent. Percent depth-dose curves were similar, but showed variations up to 3% in the buildup region. The pencil-beam algorithm (PBA) fit measured data from the eMLC and applicator-cutout systems equally well, and the resulting two-dimensional (2-D) dose distributions, as predicted by the PBA, agreed well at common airgap distance. Simulating patient setups for breast and head and neck treatments showed that almost all fields could be treated using similar SSDs as when using applicators, although head and neck treatments require placing the patient's head on a head-holder treatment table extension. The results of this work confirmed our design goals and support the potential use of the eMLC design in the clinical setting. The eMLC should allow the same treatments as are typically delivered with the electron applicator-cutout system currently used for fixed-beam therapy.
[DOI: 10.1118/1.1644516]

Key words: electron collimation, multileaf collimator, electron beam dosimetry

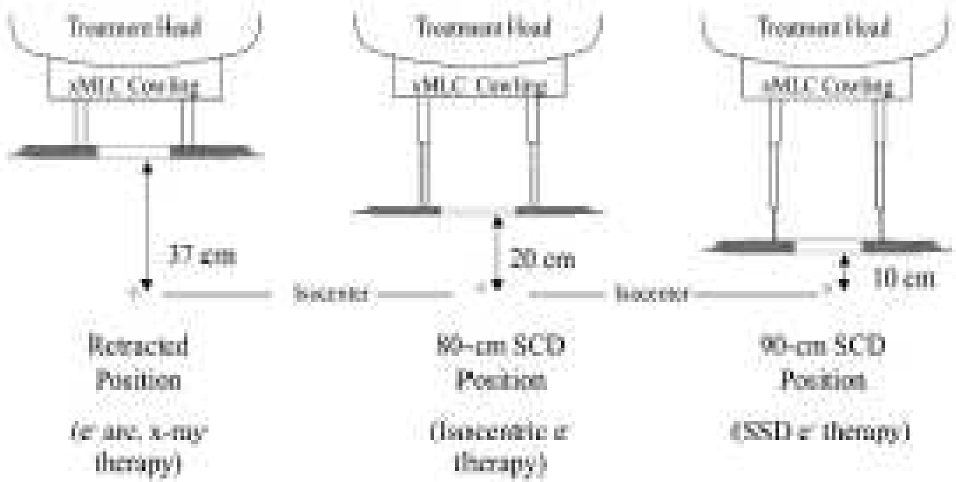

FIG. 1. Schematic design concept for a deployable–retractable eMLC. The retracted position of 63 cm SCD, distal surface of the eMLC located 37 cm from the isocenter, is intended for electron arc therapy or x-ray therapy. The deployed position of 80 cm SCD, distal surface located 20 cm from the isocenter, is intended for isocentric electron therapy. The deployed position of 90 cm SCD, distal surface located 10 cm from the isocenter, is intended for SSD electron therapy.

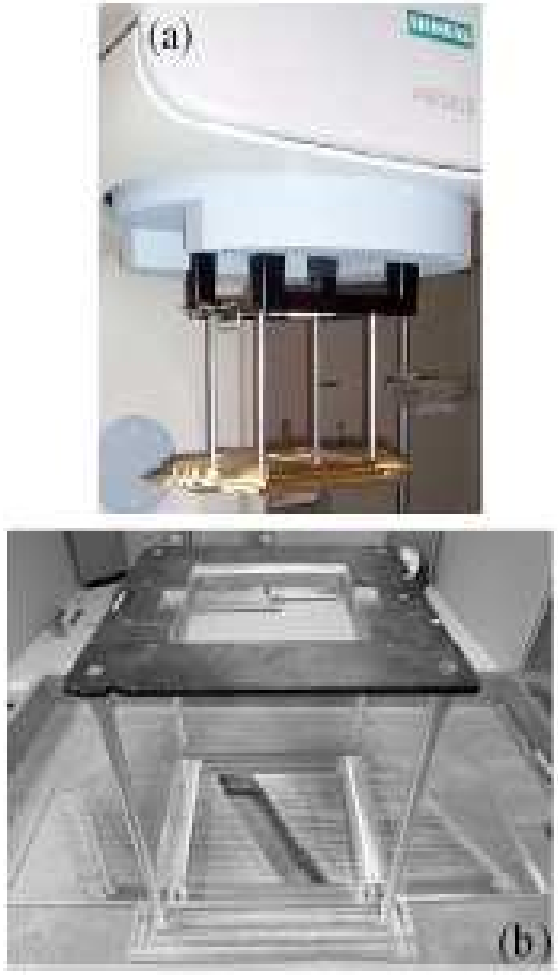

FIG. 5. (a) View of eMLC mounted on Siemens Primus accessory tray holder. Note the upper trimmer and lower leaf bed. Rigid rods placed the eMLC leaves 10 cm from the isocenter (90 cm SCD) for the present set of measurements. (b) View showing details of 21-leaf pairs. Indices on the leaf bed support and guidance plate were used for the manual positioning of leaves.

Sources of bremsstrahlung radiation in electron beams

accelerator head (sc foil & coll)

cerrobend blocks

patient

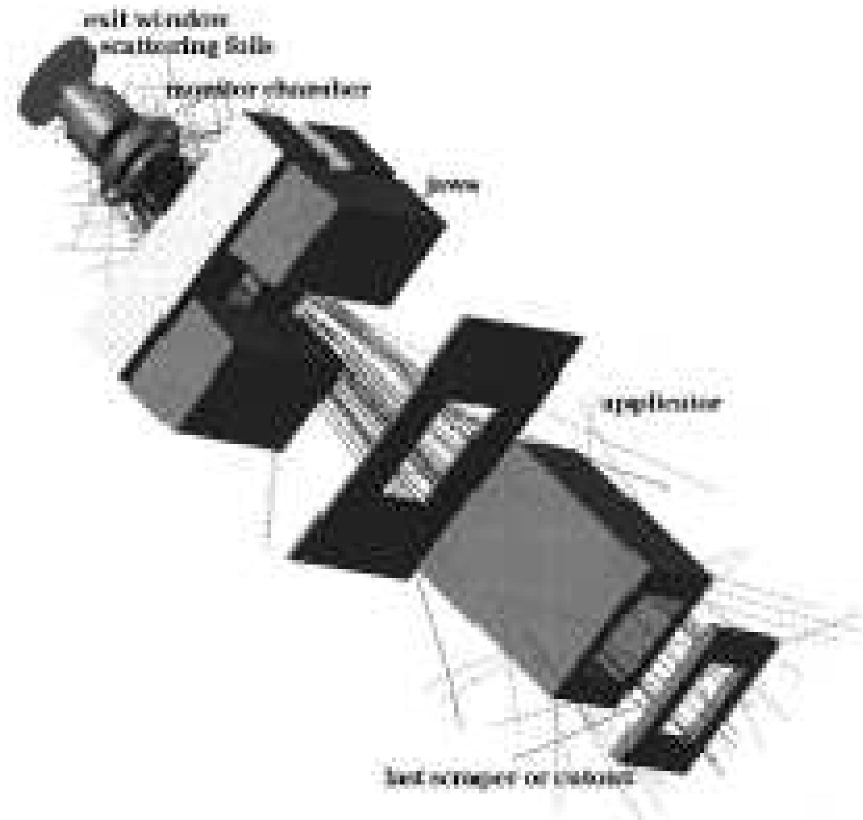

FIG. 2. The geometry of a Siemens MD2 accelerator head, and the simulated electron beam. The last scraper, corresponding to No. 5 in Fig. 1, where the cutout is inserted, is 5 cm above the phantom surface. Electrons are represented by solid lines while photons are dashed lines. In this example, there are 200 incident electrons with 10 electrons and 24 photons registered at the scoring plane which is at the phantom surface.

Analysis of the bremsstrahlung component in 6–18 MeV electron beams

Surendra N. Rustgi and James E. Rodgers
Department of Radiation Medicine, Georgetown University Hospital, Washington, D.C. 20007

(Received 30 July 1986; accepted for publication 2 February 1987)

The magnitude of the bremsstrahlung component in the 6–18 MeV electron beams from a Varian Clinac 18 accelerator was measured directly using a 0.16 T magnetic field to deflect the electron beams. The central axis depth ionization curves were measured at 130- and 197-cm source–surface distances in a Therados RFA-3 water phantom with and without the magnet being placed between the $4 \times 4\ cm^2$ electron cone and the water phantom. Results obtained clearly demonstrate that the bremsstrahlung component is primarily (> 90%) generated in the electron scattering-foil/collimation system and not in the water phantom. The x-ray central axis depth ionization curves exhibit buildup and attenuation regions characteristic of megavoltage x-ray beams. Ionization profiles of the x-ray component, measured in a plane perpendicular to the central axis, were also examined. Analysis of bremsstrahlung production as a function of photon collimation jaw opening shows a strong dependence, especially for the smaller openings.

Key words: electron beam, bremsstrahlung, dosimetry

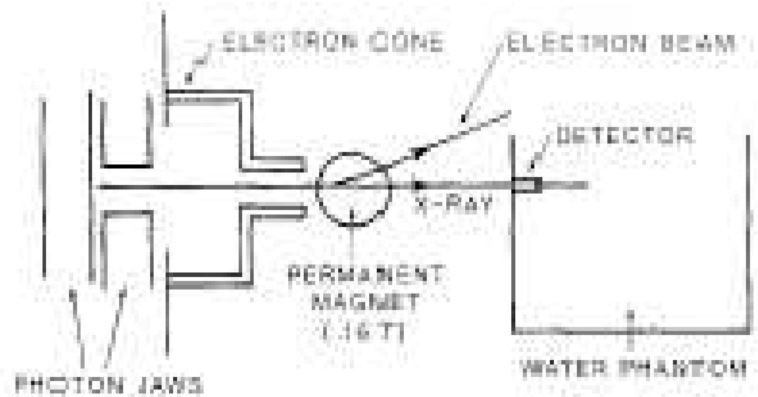

FIG. 1. Schematic of the experimental setup.

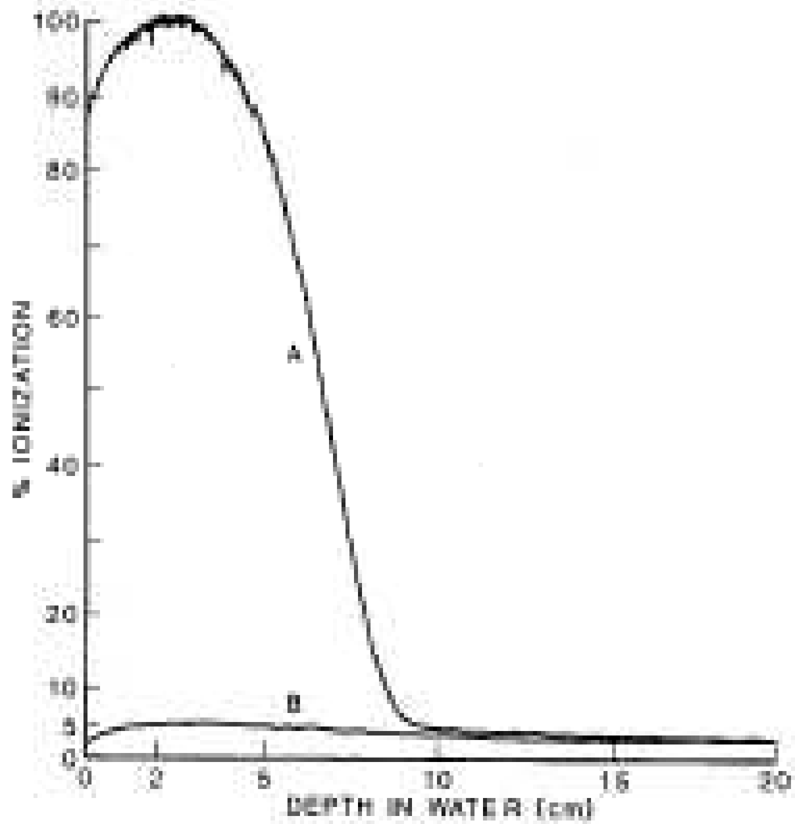

FIG. 2. Separation of accelerator generated bremsstrahlung from the total is illustrated by the typical percent ionization vs depth curves in water for an 18-MeV electron beam at 130-cm SSD. Curve A (without magnet) and curve B (with 0.16 T magnetic field). The same normalization condition was used for both curves.

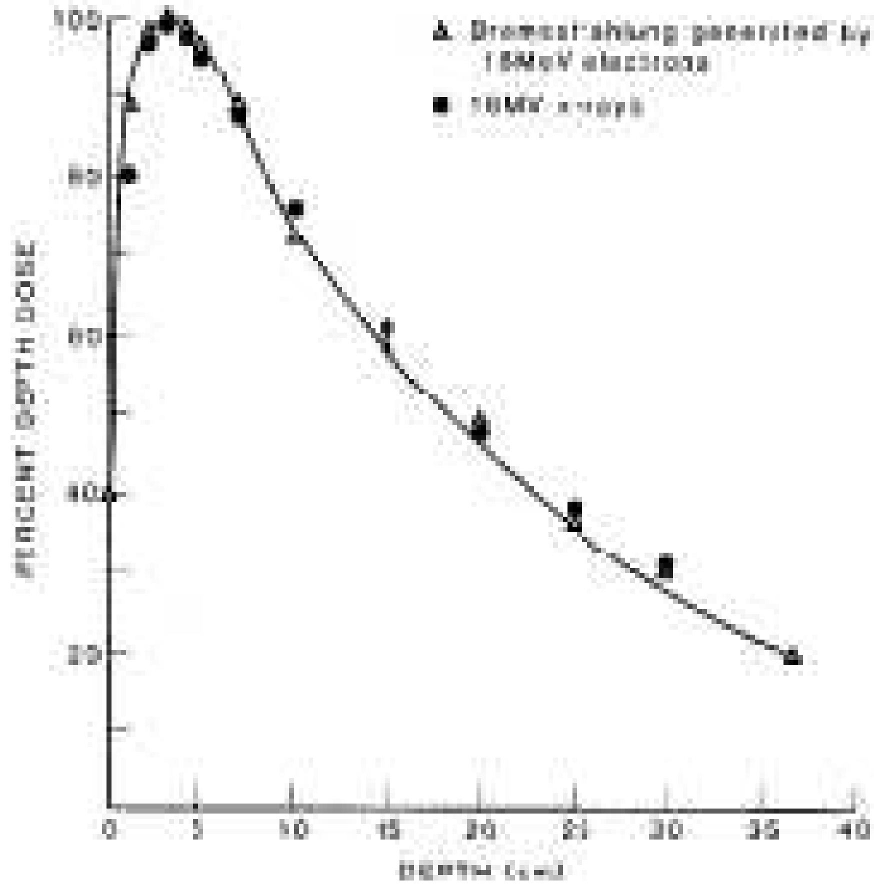

FIG. 3. Δ: Curve B from Fig. 2 for the accelerator generated x rays from the 18-MeV electron beam normalized to 100% at d_{max}. ●: Depth dose points for a 16-MV x-ray beam (Ref. 5) provided for comparison.

TABLE II. The results of the phantom generated x-ray component relative to the accelerator generated component obtained from ionization chamber measurements with and without the magnet.

Nominal electron beam energy	Measurement depth in water[a]	Phantom generated x-ray dose relative to accelerator generated x-ray dose[b]	Phantom generated x-ray dose at R_p relative to maximum electron and x-ray dose at d_{max}[b]
6 MeV	5 cm	0.040	0.0010
9	7	0.042	0.0015
12	9	0.072	0.0026
15	11	0.085	0.0034
18	14	0.098	0.0040

[a] Measurement depth is beyond the practical range and straggling distance of electrons.
[b] Measurement SSD of 130 cm.

Characteristics of bremsstrahlung in electron beams

Timothy C. Zhu,[a] Indra J. Das, and Bengt E. Bjärngard
Department of Radiation Oncology, University of Pennsylvania, Philadelphia, Pennsylvania 19104

(Received 17 November 2000; accepted for publication 18 April 2001)

Clinical electron beams contain an admixture of bremsstrahlung produced in structures in the accelerator head, in field-defining cerrobend or lead cutouts, and in the irradiated patient or water phantom. Accurate knowledge of these components is important for dose calculations and treatment planning. In this study, the bremsstrahlung components are separated for electron beams (energy 6–22 MeV, diameter 0–5 cm) using measurements in water and calculations. The results show that bremsstrahlung from the accelerator head dominates and increases with field size for electron beams generated by accelerators equipped with scattering foils. The bremsstrahlung from the field-defining cerrobend accounts for 10% to 30% of the total bremsstrahlung and decreases with increasing beam radius. The bremsstrahlung is softer than the x-ray beams of corresponding nominal energy since the latter are hardened by the flattening filter. For the 6, 12, and 22 MeV electron beams, the effective attenuation coefficients in water for the bremsstrahlung are 0.058, 0.050, and 0.043 cm^{-1}. The depths of maximum dose at 100 cm SSD are 0.8, 1.7, and 3.0 cm. The position of the virtual source of the bremsstrahlung shifts downstream from the nominal source position by 20, 13, 5.6 cm, respectively. The lateral bremsstrahlung dose distribution is more forward-peaked for higher electron energy. The bremsstrahlung components could be described for any machine by a set of simple measurements and can be modeled by an analytical expression. [DOI: 10.1118/1.1382608]

Key words: bremsstrahlung, electron beam, radiotherapy, Monte Carlo

TABLE I. Various parameters of electron beams and bremsstrahlung [Eq. (3)]. The parameter μ is the effective attenuation coefficient, and α describes rate of buildup, for bremsstrahlung photons. The factor v describes the value of surface dose $K(1.0-v)$, where K is a constant, and d_{max} is the depth of maximum dose for bremsstrahlung. D_x is the ratio of maximum bremsstrahlung dose to maximum total dose. R_p is the practical range, E_p is the most probably energy, $\bar{E}_s$ is the mean energy of the electrons at surface.

Energy	6 MeV	9 MeV	12 MeV	15 MeV	18 MeV	22 MeV
μ (cm^{-1})	0.0584	0.0538	0.0497	0.0467	0.0446	0.0431
α (cm^{-1})	1.025	1.118	1.270	1.117	0.989	0.864
v	0.194	0.366	0.428	0.479	0.489	0.491
d_{max}(cm)	0.8	1.1	1.7	2.2	2.6	3.0
K	0.010	0.018	0.030	0.051	0.074	0.121
D_x(%)	0.9	1.6	2.6	4.3	6.2	10.1
R_p(cm)	2.97	4.36	6.09	7.68	9.24	11.3
E_p(MeV)	6.1	8.9	12.4	15.6	18.7	22.8
$\bar{E}_0$(MeV)	5.7	8.5	11.9	15.0	17.7	20.7

$$d_{max} = 0.145 \; E_0$$

$$\mu(E_0) = 0.084 \; E_0^{-0.218}$$

Materials

Varian Cl 2100C – 6, 9, 12, 16 and 20 MeV electron beams

Materials attached to end of 6x6 cm^2 cone

- **brass**
- **cerrobend**
- **tungsten**
- **polyethylene**

Solid Water Phantom – RMI 451

Detectors

- **TLDs – bremsstrahlung dose**
- **EDR film – CA PDD and beam profiles**
- **Attix parallel-plate chamber – CA PDD**

Some Physical properties of the materials

material	Thickness (cm)	$\rho(g/cm^3)_{meas}$	$(\rho Z/A)_{rel\ wat}$
polyethylene	15.5	0.94	0.968
brass	3.0	8.4	6.79
cerrobend	1.7	9.4	6.79
tungsten	2.0	18	12.8

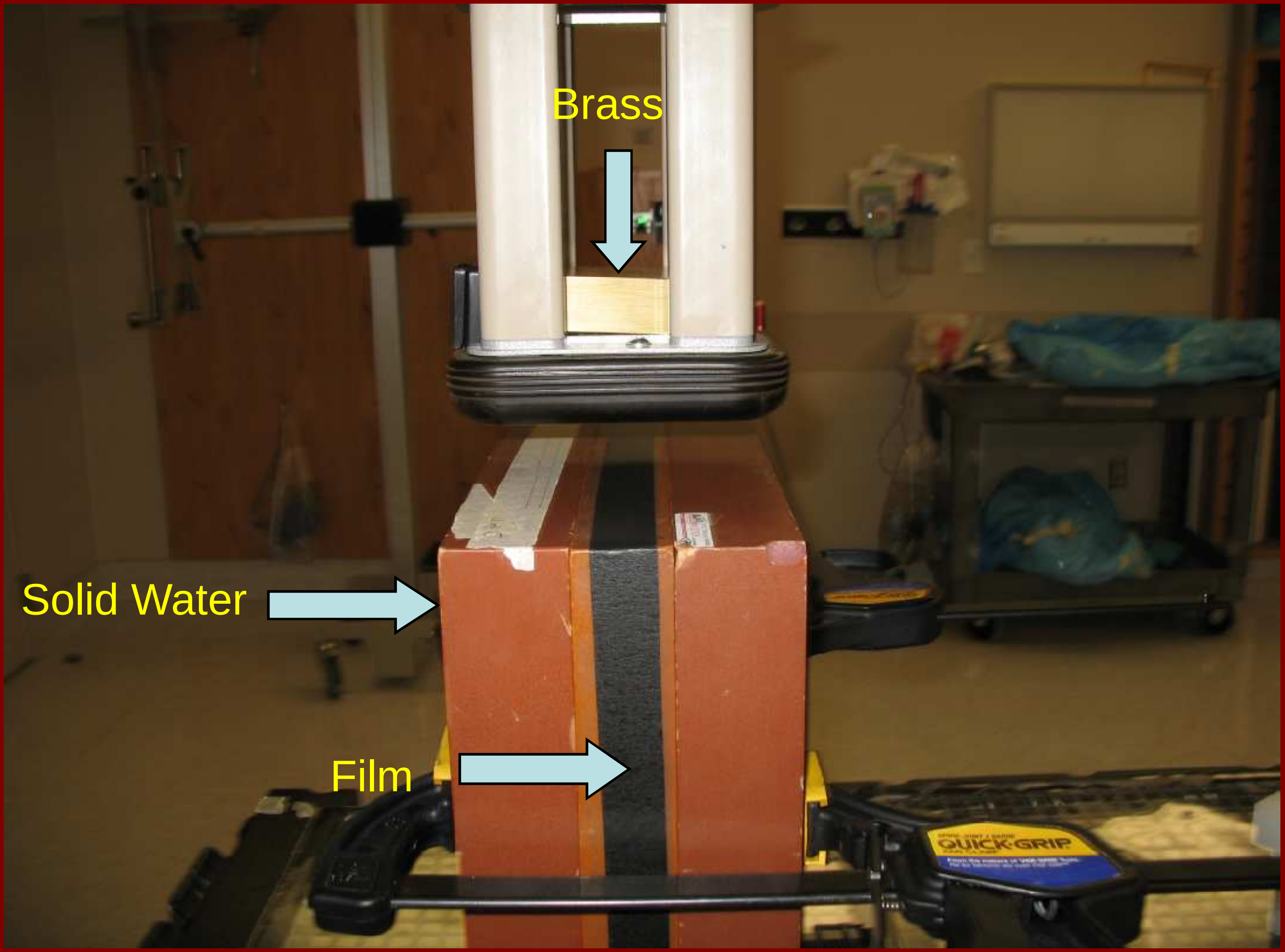
Brass
Solid Water
Film
QUICK-GRIP

Some Electron Beam Parameters

E(MeV)	R_{50}(cm)	R_p(cm)
6	2.4	2.8
9	2.7	4.5
12	6.1	6.3
16	6.8	8.4
20	8.5	10.6

Figure Summary of dose measurements at Rp+2 for the metals normalized to the dose at dmax for an open field

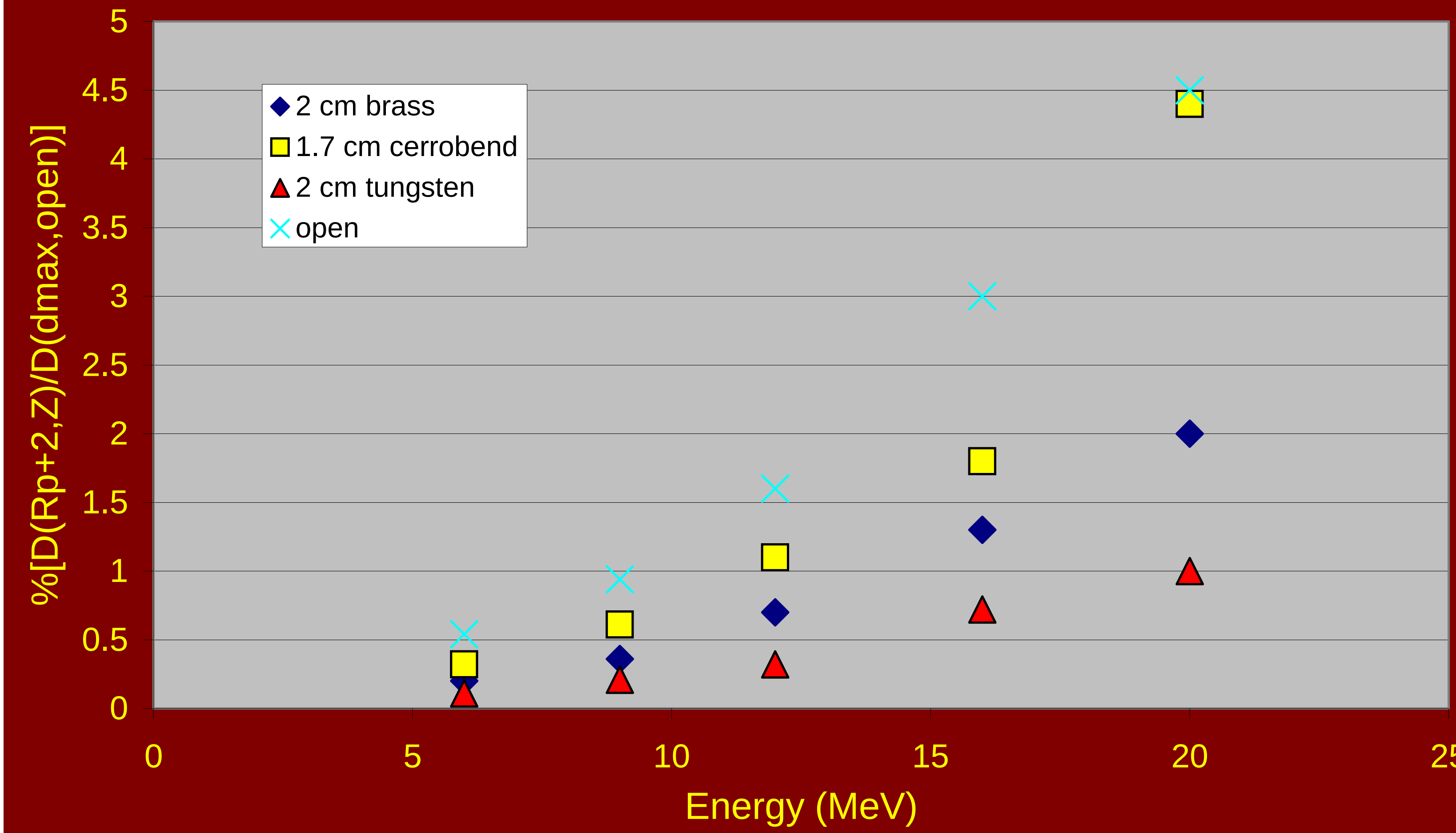

% dose at 1 cm depth for bremsstrahlung radiation produced by 20 MeV electrons incident on various materials relative to the dose for an open field at d_{max} for 20 MeV electrons

% [D_{brem}(1cm) / D_{20E}(d_{max})]				
Open#	Poly 15.5 cm	Brass 3 cm	Cerrob 1.7 cm	W 2 cm
4.9	4.7	6.1	8.5	3.5

measured at depth of R_p + 2 cm = 12.6 cm

% Dose^{block}(d=3cm) / Dose^{open}(d_{max},E)
6x6 cm^2 Cone

E(MeV) / Mat	6	9	12	16	20
Tungsten	0.20	0.30	0.60	1.4	**2.2**
Brass	0.24	0.50	1.1	2.8	**5.3**
Cerrobend	0.40	------	3.7	3.7	------
Open R_p+2cm	0.50	0.90	1.5	3.2	**4.5**

TABLE II. Predictions of the bremsstrahlung dose as a percentage of the maximum central-axis dose (electron and x ray) for the 21 MeV, 40×40 cm^2 beam on the Siemens Primus. Results are calculated using Monte Carlo calculations at a depth of 3 cm in water, which has a 100 cm SSD. The eMLC material is a slab that covers the entire beam and is located 10 cm above the water (90 cm SCD). The two locations of dose results are meant to encompass the range expected for a 20×21 cm^2 eMLC.

	Bremsstrahlung treatment head		Bremsstrahlung eMLC		Bremsstrahlung total	
eMLC material	Central axis	10 cm Off axis	Central axis	10 cm off axis	Central axis	10 cm off axis
Open beam	5%	1.5%	0%	0%	5%	1.5%
3 cm brass	2.5%	0.9%	2.5%	2.1%	5%	3.0%
2 cm tungsten	1.1%	0.4%	2.0%	1.8%	3.1%	2.2%

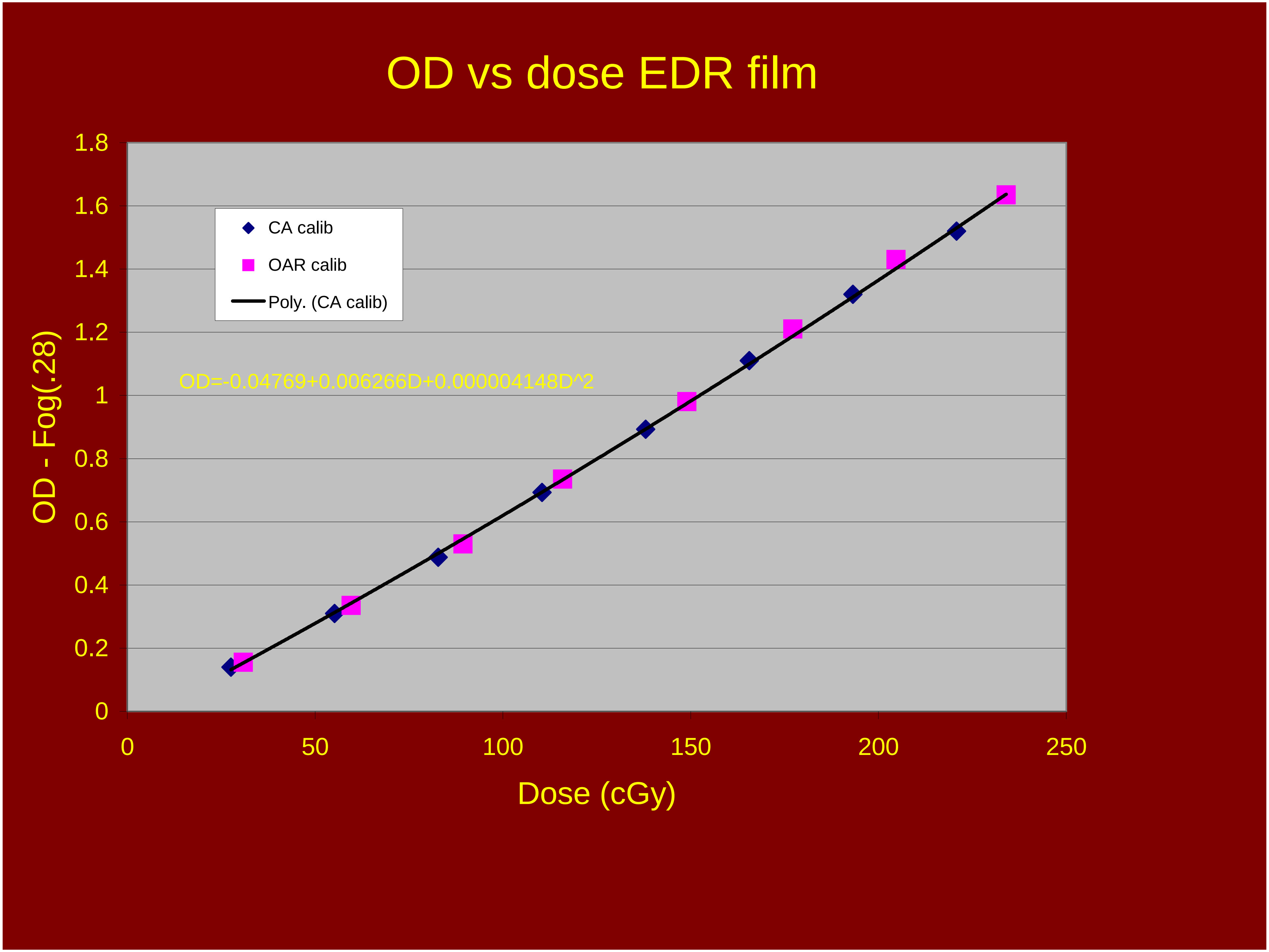

OD vs dose EDR film
CA calib
OAR calib
Poly. (CA calib)
OD=-0.04769+0.006266D+0.000004148D^2
OD - Fog(.28)
Dose (cGy)
0
0.2
0.4
0.6
0.8
1
1.2
1.4
1.6
1.8
0
50
100
150
200
250

Profiles at 1 cm depth in SW of the bremsstrahlung radiation produced by 20 MeV electrons

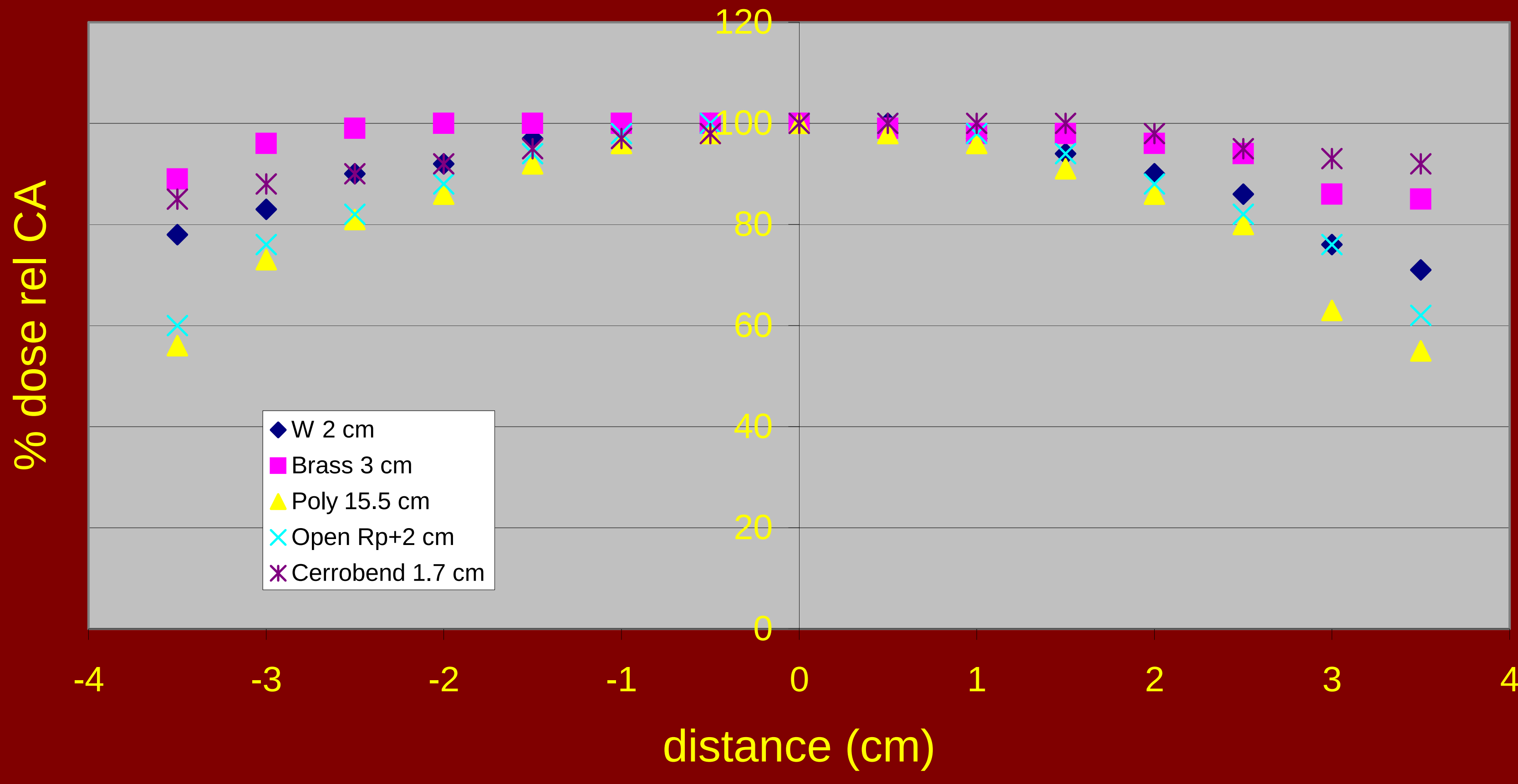

CA PDD of the bremsstrahlung produced by 20 MeV electrons incident on the materials. Note that polyethylene produces the most penetrating beam.

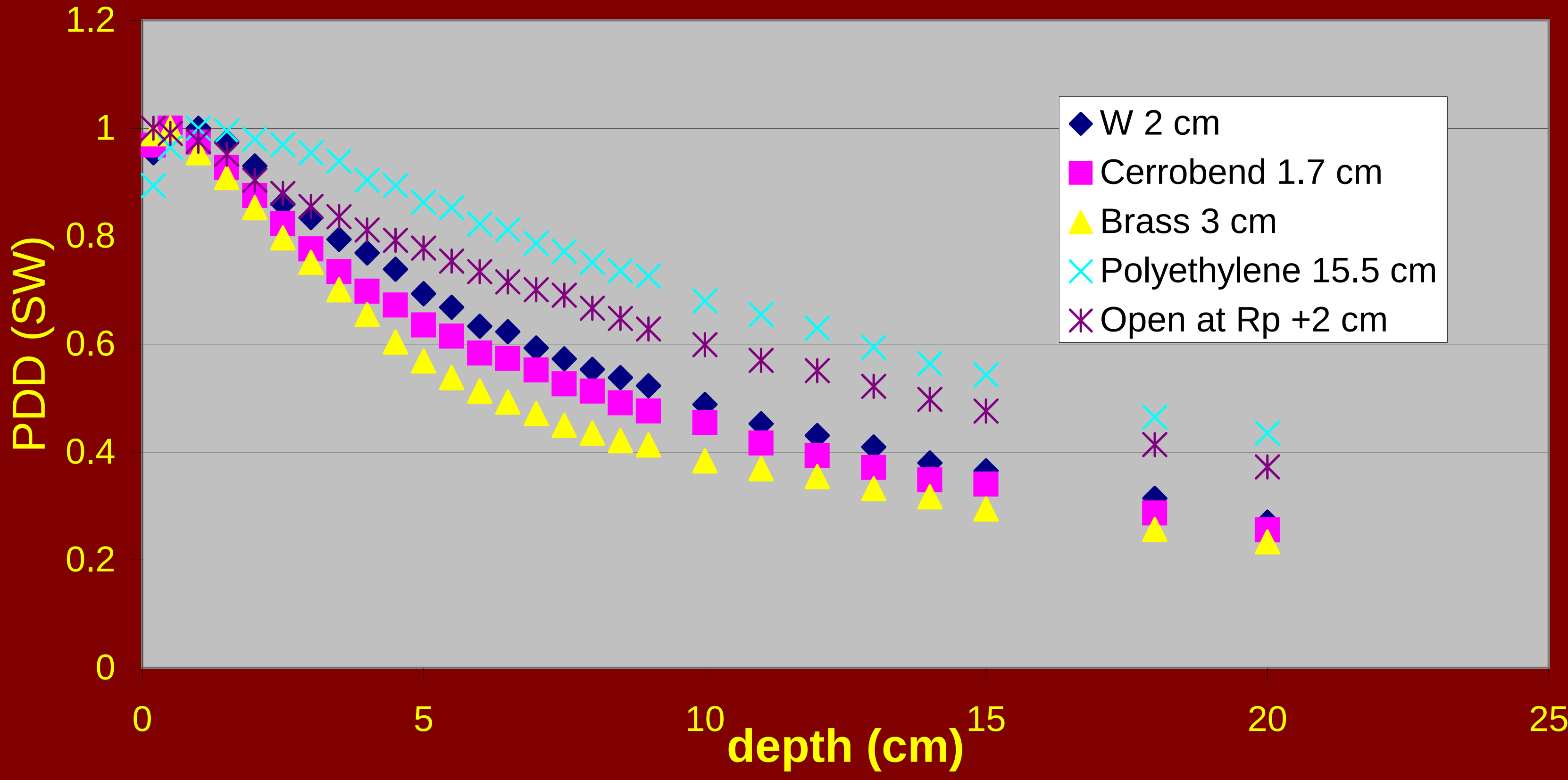

Summary of PDD in SW for the bremsstrahlung radiation Produced by 20 MeV electrons incident on various materials. Notice that polyethylene produces the most penetrating radiation

Poly 15.5 cm		Brass 3 cm		Cerrob 1.7 cm		W 2 cm	
d cm	PDD	d cm	PDD	d cm	PDD	d cm	PDD
10	68	**6.2**	**50**	**8.2**	**50**	**9.5**	**50**
16.5	**50**	10	38	10	45	10	49
20	44	20	23	20	26	20	28

DESIGN OF X-RAY TARGETS FOR HIGH ENERGY LINEAR ACCELERATORS IN RADIOTHERAPY*

By E. B. PODGORŠAK, Ph.D., J. A. RAWLINSON, M.Sc., M. I. GLAVINOVIC, B.Sc., and H. E. JOHNS, Ph.D.
TORONTO, ONTARIO, CANADA

IN a recent paper Rawlinson and Johns[9] showed that a 25 MeV linear accelerator (Varian Clinac-35) produced an inferior beam of photons to a 25 MeV betatron (Allis Chalmers). In fact, from a depth dose point of view, the linac's beam was equivalent to the beam produced by the betatron when it was operated at 16 MeV. The reasons for this were attributed to differences in the design of the target and the flattening filter in the 2 machines. The betatron employs a thin tungsten target and an aluminum flattening filter, while the linac, a thick tungsten target and a tungsten flattening filter.

The purpose of this paper is to present the experimental results of our further investigation of this problem and to suggest some methods for improving the x-ray beams from linacs used in radiotherapy. In the present experiments the 25 MeV electron beam from the linear accelerator was used to produce x-rays in targets of different atomic numbers. The x-ray beams were flattened with flattening filters made of various materials. Using these targets and filters, depth doses and x-ray yields were measured both along the central axis of the beam and at different angles to the central axis.

We have found that by using a *thick aluminum* target and an *aluminum flattening filter* in the linear accelerator we can obtain the same depth dose distribution as from the Allis Chalmers betatron operating at the same energy. Furthermore, the x-ray yield in the forward direction is the same within a few per cent, whether we use a thick aluminum or thick lead target. It thus appears that thick targets in linear accelerators should be made of low atomic number materials. For such targets a more penetrating beam is produced and the yield in the forward direction is as good as from a high atomic number material.

EXPERIMENTAL APPARATUS AND PROCEDURES

Experiments reported in this paper have been carried out at the Ontario Cancer Institute in Toronto using the electron beam from a Varian Clinac-35 linear accelerator. The schematic diagram of the experimental apparatus is shown in Figure 1. As normally used in radiotherapy, the electron beam is bent first through 57°, next focused by 2 quadrupole lenses, and then bent 90° to hit a tungsten target where it produces an x-ray beam which emerges at port No. 3. This port was not used in our experiments because of the difficulties in removing the linac head (collimators, transmission ion chamber, etc.) to obtain an unobstructed electron beam. Instead, in our studies we turned off the 90° bending magnet allowing the electron beam to emerge at port No. 2 through a thin beryllium window. The extracted electron beam was then made to produce x-rays in our own targets which were secured to the linac in the position shown in the diagram. With the 90° bending magnet turned off, the electron beam was focused onto the target into a circle of ~3 mm diameter. The experimental apparatus will be discussed in more detail in the following sections.

TARGETS

The targets were cylinders of 5 cm diameter positioned in air 3 cm from the beryllium exit window. Their thicknesses

* From the Physics Division, Ontario Cancer Institute, Toronto, Ontario, Canada.

DESIGN OF X-RAY TARGETS FOR HIGH ENERGY LINEAR ACCELERATORS IN RADIOTHERAPY

E. B. PODGORŠAK PH.D., J. A. RAWLINSON M.SC., M. I. GLAVINOVIĆ B.SC., and H. E. JOHNS PH.D.

The 25 MeV electron beam was extracted from a Varian Clinac-35 linear accelerator and made to produce x-rays in thick targets of different materials. The x-ray beams were flattened by filters of various materials.

We have found that an aluminum thick target gives a more penetrating beam in the forward direction than does a lead or tungsten target.

The x-ray yield in the forward direction from 0-5° is essentially the same for both aluminum and lead targets. At angles larger than 10°, a lead target shows a higher x-ray yield and a more penetrating beam than an aluminum target.

The flattening filter material is important. A more penetrating beam is produced if the flattening filter is made of aluminum rather than tungsten or lead.

With an aluminum target and an aluminum flattening filter, we obtain the same depth dose distribution from our linear accelerator as we do from our betatron unit operating at the same energy. In the betatron unit, the radiation is produced in a thin target of tungsten and filtered by aluminum.

For the situations that arise in radiotherapy we have shown that the beam from an aluminum target/aluminum flattening filter combination can be flattened just as easily as the beam from a lead target/lead flattening filter combination.

We conclude, therefore, that contrary to conventional practice, low atomic number materials should be used for the targets and flattening filters of high energy radiotherapy linear accelerators.

We plan to extend our investigations of target and filter design to lower electron energies (10-20 MeV).

Summary of PDD in SW for the bremsstrahlung radiation Produced by 6 MeV electrons incident on polyethylene and W. The beam qualities are very similar.

Polyethylene 5.8 cm		W 0.5 cm	
d cm	PDD	d cm	PDD
8.2	50	8.0	50
10	43	10	43

CONCLUSIONS

1. These results show that 2 cm thick W stops 20 MeV electrons while reducing the x-ray dose to a level lower than that produced in the open field – 1% compared to 4.5%.

2. The most penetrating bremsstrahlung radiation was measured for the electrons on polyethylene, the lowest Z material. This is consistent with the work of Podgorsak et al[3] which showed that at these beam energies the more penetrating radiations is produced in the lower Z material.

3 These results provide measurements to compare with Monte Carlo calculations The % central-axis dose (electron and photon) for 20 MeV electrons at 3 cm depth for open, brass and W are 4.5, 5.3 and 2.3% respectively, in reasonable agreement with the published Monte Carlo calculations[3] of 5,5 and 3.1% for 21 MeV electrons.

OD vs dose EDR film

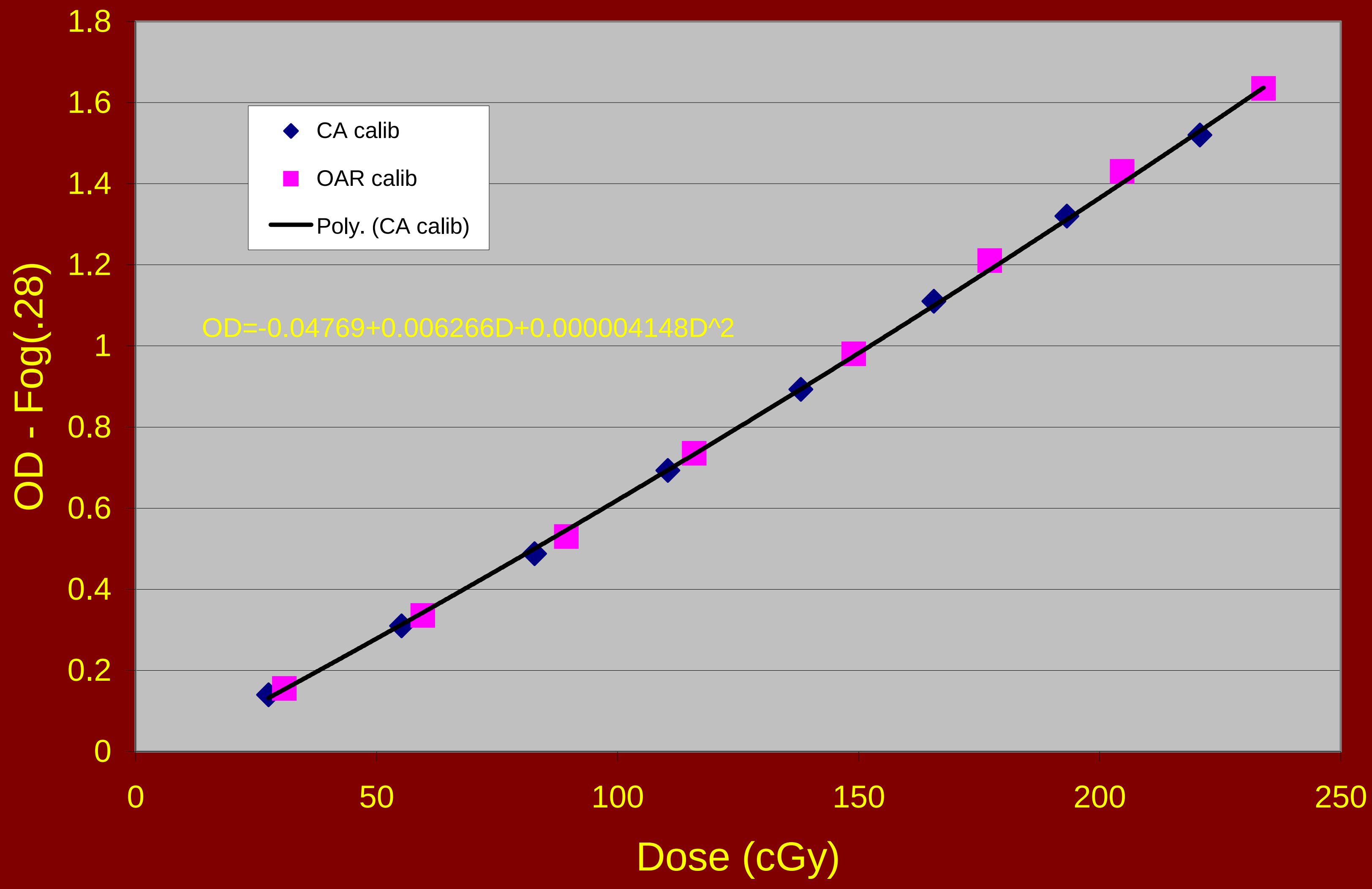

Profiles at 1 cm depth in SW of the bremsstrahlung radiation produced by 20 MeV electrons incident on the materials

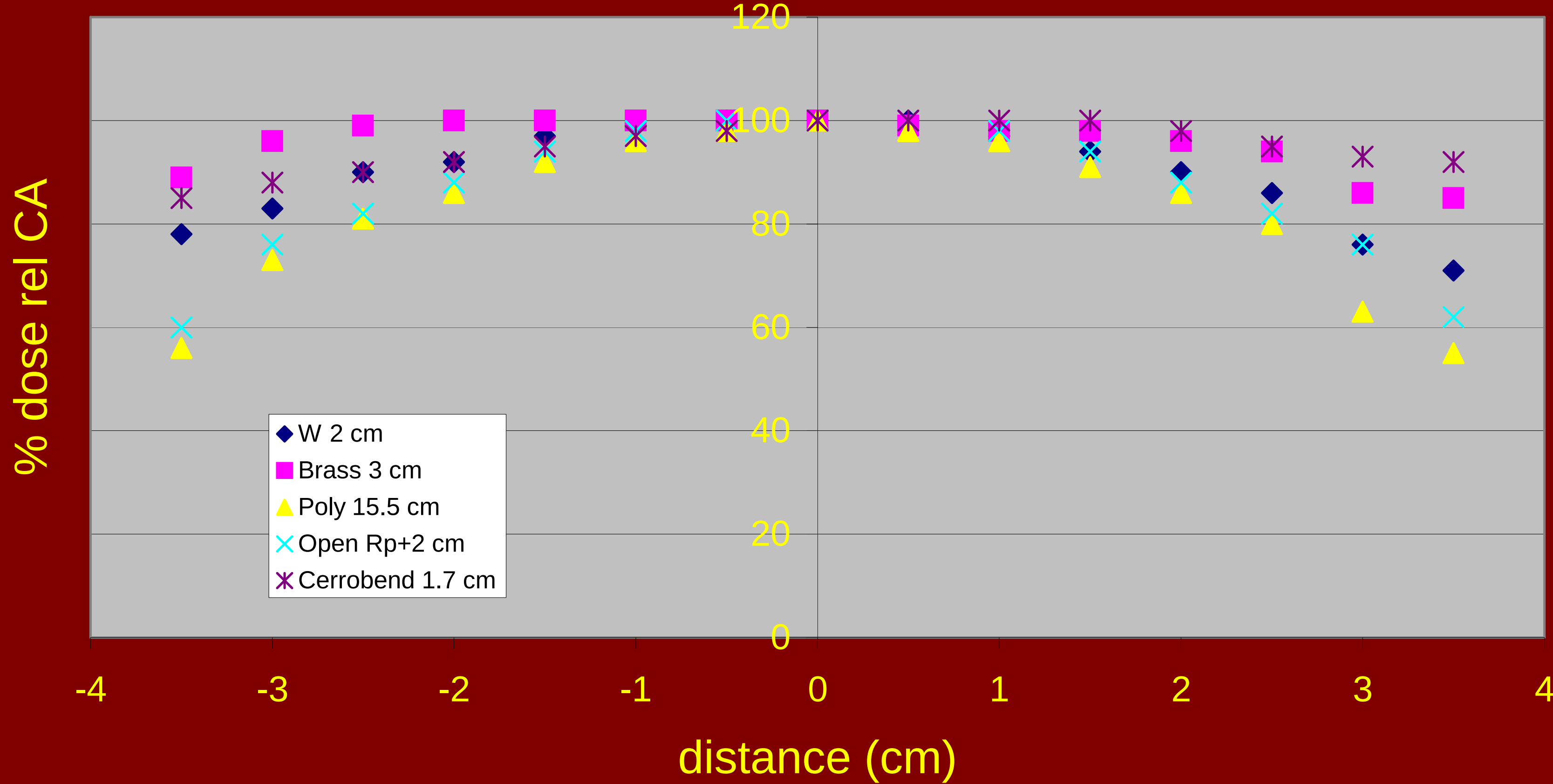

PDD of the bremsstrahlung produced by 20 MeV electrons incident on materials

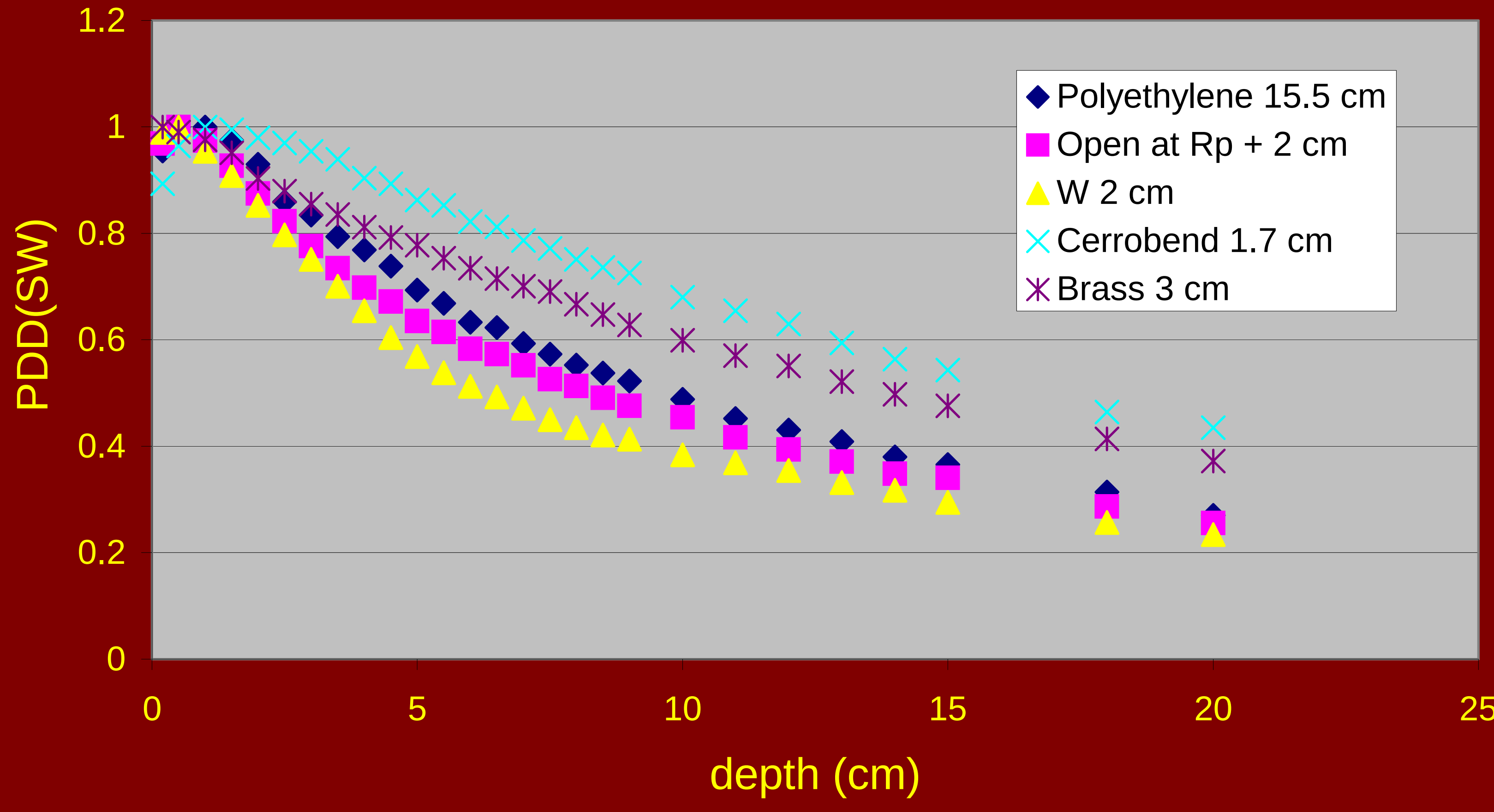

Summary of PDD in SW for the bremsstrahlung radiation Produced by 20 MeV electrons incident on various materials

Open[#]		Poly 15.5 cm		Brass 3 cm		Cerrob 1.7 cm		W 2 cm	
d cm	PDD	d cm	PDD	d cm	PDD	d cm	PDD	d cm	PDD
10	60	10	68	**6.2**	**50**	**8.2**	**50**	**9.5**	**50**
14	**50**	**16.5**	**50**	10	38	10	45	10	49
20	37	20	44	20	23	20	26	20	28

[#] Rp + 2 cm

Summary of dose measurements at Rp+2 for the bremsstrahlung produced in metals relatiave to the dose at dmax for an open field

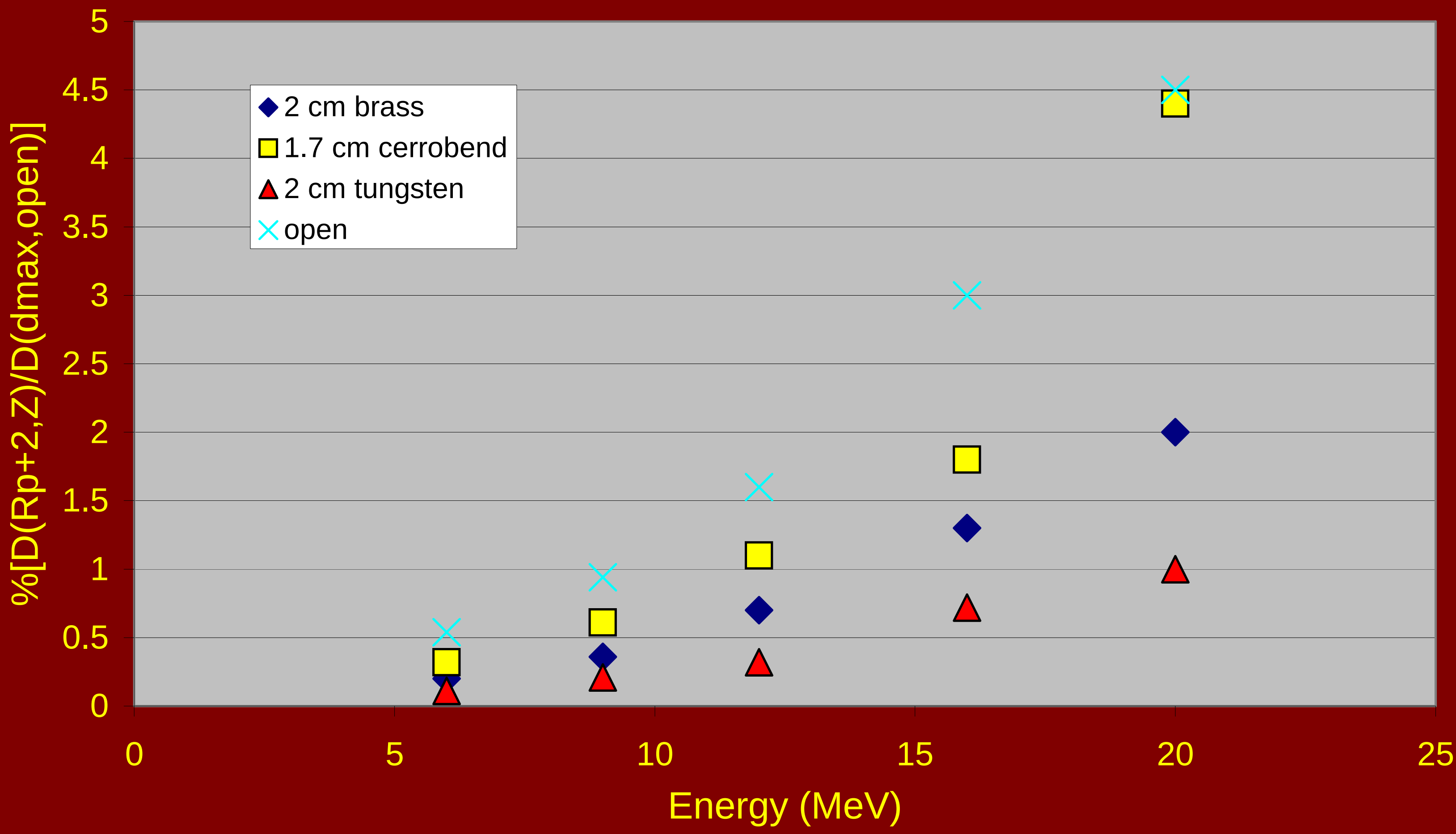

CA PDD of the bremsstrahlung produced by 20 MeV electrons incident on the materials. Note that polyethylene produces the most penetrating beam.

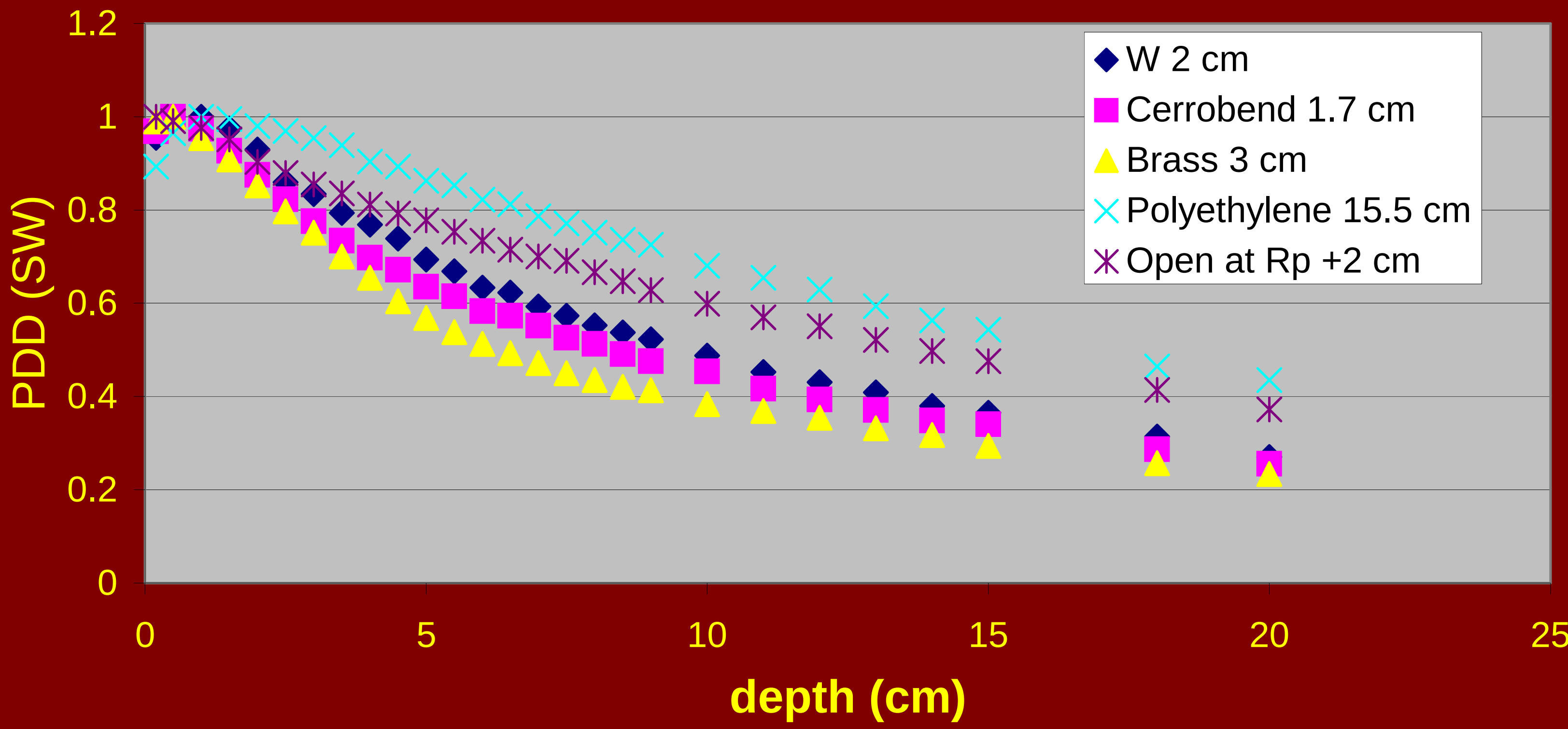

Abstract

Bremsstrahlung radiation in electron beams is produced in the accelerator head (scattering-foil and collimators), the cerrobend or field defining devices and within the patient. The dominate contribution comes from the head[1]. However, in areas shielded by electron multileaf collimators the bremsstrahlung produced in the collimating leaves will be significant. Here the total bremsstrahlung dose is measured for megavoltage electron beams incident on three metals used to simulate the collimating leaves in a multileaf collimator. Beam profiles at 1 cm depth are obtained as well as percentage depth dose measurements to estimate the beam quality of the radiation distal to the materials. Some results show good agreement with published Monte Carlo calculations[2]

Materials and Methods

A Varian CI 2100C is used to provide 6, 9, 12, 16 and 20 MeV electron beams. At the end of the standard 6x6cm^2 cone are positioned materials of appropriate thickness to simulate the multileaves. The materials studied are brass, cerrobend and tungsten. Although polyethylene is not practical for use as multileaves, it is included because it is similar to the bremsstrahlung for an open field and also to compare with the radiation quality from the higher z metals. Thermoluminescent dosimeters (0.089 cm thick by 0.32x0.32 cm^2), EDR film and an Attix parallel-plate ionization chamber are used to measure the central axis x-ray dose in a solid water (RMI 451) phantom at a source-to-surface distance of 100 cm. Film oriented parallel to the beam is used to obtain beam profiles at 1 cm depth and also the central-axis percentage depth dose to estimate the beam quality of the bremstrahlung spectra.